2019

In-fiber temperature sensor based on green up-conversion luminescence in an Er3+-Yb3+ co-doped tellurite glass microsphere

Meng Zhang

Angzhen Li

Jibo Yu

See next page for additional authors

Funder: National Key R&D Program of China; National Natural Science Foundation of China (NSFC); Harbin Engineering University; Fundamental Research Funds for the Central Universities; Open Fund of the State Key Laboratory on Integrated Optoelectronics

Authors

Meng Zhang, Angzhen Li, Jibo Yu, Xiaosong Lu, Shunbin Wang, Elfed Lewis, Gerald Farrell, Libo Yuan, and Pengfei Wang

In-fiber temperature sensor based on green up-conversion luminescence in an Er 3+ –Yb 3+ co-doped tellurite glass microsphere

Article *in* Optics Letters · July 2019

DOI: 10.1364/OL.44.003214

9 authors, including:

Meng Zhang
Harbin Engineering University
18 PUBLICATIONS **103** CITATIONS
SEE PROFILE

Angzhen Li
Harbin Engineering University
20 PUBLICATIONS **85** CITATIONS
SEE PROFILE

Yu Jibo
Harbin Engineering University
19 PUBLICATIONS **106** CITATIONS
SEE PROFILE

Xiaosong Lu
Jiangsu Normal University
25 PUBLICATIONS **272** CITATIONS
SEE PROFILE

Optics Letters

In-fiber temperature sensor based on green up-conversion luminescence in an Er^{3+}-Yb^{3+} co-doped tellurite glass microsphere

Meng Zhang,[1] Angzhen Li,[1] Jibo Yu,[1] Xiaosong Lu,[1] Shunbin Wang,[1] Elfed Lewis,[2] Gerald Farrell,[3] Libo Yuan,[1] and Pengfei Wang[1,4,*]

[1]Key Lab of In-Fiber Integrated Optics, Ministry of Education of China, Harbin Engineering University, Harbin 150001, China
[2]Optical Fibre Sensors Research Centre, Department of Electronic and Computer Engineering, University of Limerick, Limerick V94 T9PX, Ireland
[3]Photonics Research Centre, Dublin Institute of Technology, Kevin Street, Dublin 8, Ireland
[4]Key Laboratory of Optoelectronic Devices and Systems of Ministry of Education and Guangdong Province, College of Optoelectronic Engineering, Shenzhen University, Shenzhen 518060, China
*Corresponding author: pengfei.wang@dit.ie

Received 5 February 2019; revised 14 May 2019; accepted 18 May 2019; posted 24 May 2019 (Doc. ID 359142); published 17 June 2019

A novel, to the best of our knowledge, in-fiber temperature sensor based on green up-conversion (UC) luminescence in an Er^{3+}-Yb^{3+} co-doped tellurite glass microsphere is described. The tellurite glass microsphere is located firmly inside a suspended tri-core hollow-fiber (STCHF) structure. The pump light launched via a single-mode fiber (SMF) is passed through a section of multimode fiber, which is fusion spliced between the SMF and the STCHF into the cores suspended inside the hollow fiber and coupled into the microsphere. Green and red UC emissions of the Er^{3+} ions are observed using 980 nm pump excitation. The temperature-sensing capability of the tellurite glass microsphere is based on the thermally coupled effect between the upper energy levels responsible for green emissions at 528 nm and 549 nm. The resulting fluorescence intensity ratio, depending on the surrounding temperature range from 303 K to 383 K, is experimentally determined, and a maximum sensitivity of 5.47×10^{-3} K^{-1} is demonstrated. This novel in-fiber microsphere-resonator-based device is highly integrated and has the additional advantages of ease of fabrication, compact structure, and low fabrication cost and therefore has great application potential in integrated optical sources including lasers.

https://doi.org/10.1364/OL.44.003214

Rare-earth (RE^{3+})-doped materials have recently been widely studied and used in photonics with wide applicability in solid-state lasers and optical amplifiers, which require high emission quantum yields [1–5]. Among the multiple applications found for RE^{3+}-doped materials, up-conversion (UC) luminescent emission has a significant role to play for temperature sensors [6,7]. These optical sensors are based on the temperature-dependent fluorescence intensity ratio (FIR) technique using RE^{3+} materials doped in different host materials [8–10], which takes advantage of the temperature-dependent emission intensities of two thermally coupled emitting levels of the RE^{3+} ions. The energy separation of the thermally coupled levels must be between 200 cm^{-1} and 2000 cm^{-1}, which not only prevents strong overlapping of the two emissions but also allows the upper level to have a minimum population of optically active ions in the temperature range of interest (in this case, 303–383 K) [11,12]. Er^{3+} as a dopant has been the most widely studied material for optical sensors, as it exhibits strong UC fluorescence emissions upon excitation using near-infrared (NIR) radiation. The emissions are greatly enhanced if Yb^{3+} is co-doped in the Er^{3+}-doped materials, as it is known to increase the absorption cross section for NIR excitation [13,14]. Different doping concentrations also affect the temperature sensitivity [15]. Alternative doped glass matrixes have also been studied for this purpose, such as chalcogenide [14], fluoroindate [9], fluorophosphate [16], tellurite [17], and fluorotellurite glasses [18]. These glass materials have demonstrated behavior used as a probe for measuring temperature based on a thermally coupled pair of energy levels of Er^{3+}, namely $^2H_{11/2}$ and $^4S_{3/2}$, whose green emission intensity ratio varies with temperature. In the work referenced above, the glass composition was initially studied in order to obtain the strongest UC fluorescence emissions by changing the ratio of RE^{3+} ions in the matrix material, and then the temperature-sensing characteristic of the glass material was characterized by means of changing the luminescence intensity with temperature. However, the excitation of the pump source and the collection of the light signal were achieved by spatial alignment, which is susceptible to a wide range of interference from environmental parameters such as humidity, mechanical vibration, etc. Recently, an optical thermometer probe comprising an Er^{3+}-Yb^{3+} co-doped tellurite glass attached to the tip of an optical fiber and optically coupled to a laser source and a portable USB spectrometer was proposed [19]. Although offering

an improvement in stability, the structure is complex and expensive, and furthermore is difficult to fabricate based on the available range of RE^{3+}-doped materials. In recent years, significant research effort has resulted in the emergence of microcavities as realistic candidates for optical resonators due to their compact structure and excellent optical performance, e.g., potentially high gain. In addition, the fabrication technology for multi-component microspheres is very mature, and hence microsphere resonators are widely used in various optical fields making use of many optical effects, e.g., whispering gallery mode (WGM), generated using optical fiber coupling [20–22]. In previous work by some of the authors of this article, a structure was fabricated and experimentally demonstrated in which a silica microsphere was encapsulated inside a special fiber, called embedded dual-core hollow fiber (EDCHF), and temperature-sensing capability was measured [23]. The work of [23] clearly demonstrated that it was feasible to make such micro-structured optical temperature sensors simpler, less expensive, more integrated, and then more widely used. Therefore, in the novel approach presented in this paper, the RE^{3+}-doped microsphere replaces the traditional silica microsphere inside the special fiber, being directly pumped using the NIR source, and hence it is possible to achieve temperature sensitivity based on the FIR of the RE^{3+}-doped microsphere.

In the investigation described in this paper, an in-fiber temperature sensor is described based on green UC luminescence in an Er^{3+}-Yb^{3+} co-doped tellurite glass microsphere. The selected host is tellurite glass, which has a relatively low phonon energy (750 cm^{-1}) and high solubility of RE^{3+}, and is highly transparent in the visible region (380–720 nm). The multiple advantages of the properties of tellurite glass result in a low multi-phonon relaxation rate for ion excitation, which has a strong impact on the energy transfer process and improves stability for the microsphere's synthesis process. The Er^{3+}-Yb^{3+} co-doped tellurite glass was initially ground into powder, then the powder was poured into a vertical furnace to prepare the microspheres. The prepared microsphere was placed inside the suspended tri-core hollow fiber (STCHF), resulting in a robustly packaged integrated device, as shown in Fig. 1. Strong green UC fluorescence emissions were observed when subject to excitation from the NIR pump light source, and the temperature measurement capability of the resulting device was tested. This low-cost and readily prepared device is expected to be well suited for use in other optical fields including lasers and novel light sources.

The Er^{3+}-Yb^{3+} co-doped tellurite glass samples ($72TeO_2$ – $20ZnO$ – $5Na_2CO_3$ – $1.5Y_2O_3$ – $0.5Er_2O_3$ – $1Yb_2O_3$) were prepared using a conventional melt-quenching method. The commercially available raw materials used were TeO_2, ZnO, Na_2CO_3, Y_2O_3, Er_2O_3, and Yb_2O_3 powders with 99.9% or higher purity. The materials were melted at 900°C for 40 min in a muffle furnace. Then, the glass melts were cast into a preheated stainless-steel mold, annealed at 350°C for 3 h, and slowly cooled to room temperature to minimize residual internal stress. Finally, the prepared tellurite glass was ground into powder and passed through a 300 mesh sieve. Large amounts of fine powders were dropped through an inert-gas-purged vertical furnace, where those powders were molten and transformed into microspheres by surface tension. To fabricate high-quality microspheres, the furnace temperature and the flow rate of the inert gas needed to be set at their optimal values, which were experimentally determined to be 800°C and 2 L/min, respectively. The microspheres fell from the hot zone in the furnace into the cold zone, where they cooled and solidified. They were then collected in a Petri dish attached to the end of a quartz tube. The Petri dish contained a small amount of deionized water, which acted as a liquid seal, stabilizing gas pressure, as well as providing the microspheres a relatively clean environment in which they could not easily be contaminated and thus avoiding a potential reduction of the achievable Q-factor. The microspheres were then transferred onto a glass slide.

Figure 2(a) shows a micrograph of the microspheres fabricated in this investigation, and it is observed that they have a very regular circular cross section, are uniform in size, and possess a smooth surface. In the next processing step, a single microsphere, with a diameter of about 50 μm, was optically coupled to a tapered fiber with diameter 1.7 μm to facilitate light input and output. The light from a super-continuum source was coupled into the microsphere through one end of the tapered fiber, and this excited the WGMs of the microsphere. The transmission spectrum at the opposite end of the fiber was measured using an optical spectrum analyser (OSA, YOKOGAWA, AQ-6370C), and the Q value was calculated to be 2.51×10^4, as shown in Fig. 2(b).

In our previous work [23], a silica microsphere was successfully located within an EDCHF. However, in this investigation, the STCHF was the preferred choice as a host fiber, as it offers the capability of achieving a more mechanically stable and reliable positioning of the microsphere due to its inherent tri-core structure distributed in an equilateral triangle shape,

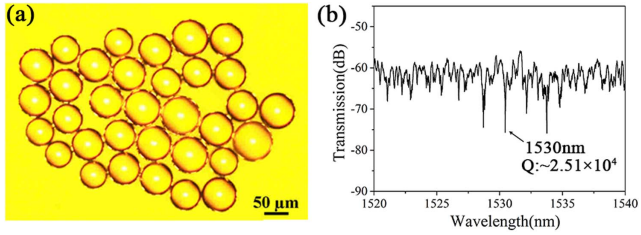

Fig. 2. (a) Microscope image of the Er^{3+}-Yb^{3+} co-doped tellurite glass microspheres fabricated in our lab and (b) transmission spectrum measured for a typical 50 μm microsphere at room temperature.

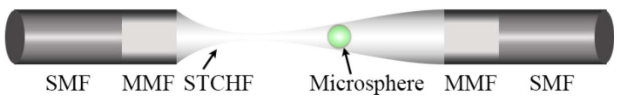

Fig. 1. Schematic of the microsphere-embedded SMF-MMF-STCHF-MMF-SMF structure.

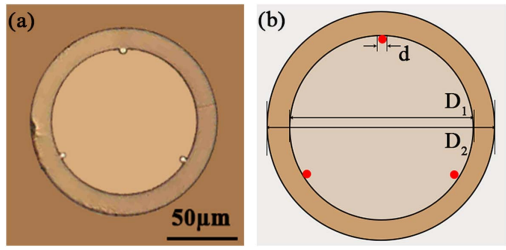

Fig. 3. (a) Microscope image of the cross section of the STCHF; (b) schematic diagram of the STCHF structure.

which naturally self-positions circular objects. Figure 3 is a schematic cross-sectional diagram of the fiber. The optical fiber consists of three circular cores with a diameter $d = 4$ μm, a central air hole with diameter $D_1 = 80$ μm, and an annular cladding with an outer diameter $D_2 = 125$ μm. A section of multimode fiber (MMF) with a core diameter of 105 μm was fusion spliced between the single-mode fiber (SMF) and the STCHF to reduce potential loss of pump light propagating through the structure. The STCHF was tapered to reduce the diameter of the cores suspended inside its air hole, thereby increasing the evanescent field surrounding the cores. The fabrication method used for tapering the STCHF and placing the microsphere inside the hollow fiber are described in detail in [22]. In the investigation described in this article, the specific fusion parameters were slightly different due to the different fiber structures involved, but the method is broadly the same. Following multiple experimental adjustment of the operating parameters, a microsphere with a diameter of about 50 μm was firmly placed in the air hole. Finally, the opposite end of the STCHF was fusion spliced to the MMF, and the microsphere was therefore encapsulated inside the fiber structure.

Figure 4 shows the energy level diagram of Er^{3+} and Yb^{3+} under 980 nm laser excitation and the associated transition mechanisms. The green UC emissions of the Er^{3+} ions are explained as follows. Above all, by absorbing the 980 nm pump light, the ground state $^4I_{15/2}Er^{3+}$ ions transition to the excited state $^4I_{11/2}$, viz., ground state absorption (GSA). The excited Er^{3+} ions in $^4I_{11/2}$ can absorb a second 980 nm photon and hence reach the highest excited state $^4F_{7/2}$, namely, the excited state absorption (ESA) process. By means of such a two-photon-assisted process, many Er^{3+} ions originally in the ground state transition to the highest excited state and then decay via a non-radiative transition to the lower excited $^2H_{11/2}$ and $^4S_{3/2}$ levels and finally produce the green emissions at 528 nm ($^2H_{11/2} \rightarrow {}^4I_{15/2}$) and 549 nm ($^4S_{3/2} \rightarrow {}^4I_{15/2}$), respectively. Additionally, there exist energy transfer (ET) processes from Yb^{3+} to Er^{3+}, $^2F_{5/2}(Yb^{3+}) + {}^4I_{15/2}(Er^{3+}) \rightarrow {}^2F_{7/2}(Yb^{3+}) + {}^4I_{11/2}(Er^{3+})$ and $^2F_{5/2}(Yb^{3+}) + {}^4I_{11/2}(Er^{3+}) \rightarrow {}^2F_{7/2}(Yb^{3+}) + {}^4F_{7/2}(Er^{3+})$, which result in more Er^{3+} existing in the excited state and thus enhancing the UC emission. Moreover, a cross-relaxation (CR) mechanism in Er^{3+} ions existing in the $^4I_{11/2}$ state, $^4I_{11/2} + {}^4I_{11/2} \rightarrow {}^4I_{15/2} + {}^4F_{7/2}$, may also occur [24]. In a similar way, excited Er^{3+} ions existing in the $^4I_{11/2}$ non-radiative transition to $^4I_{13/2}$ and absorb a second 980 nm photon to reach the $^4F_{9/2}$ state. Additionally, Er^{3+} ions undergo a non-radiative transition to $^4F_{9/2}$ from $^4S_{3/2}$ and ultimately produce the red emission at 660 nm. It is possible to achieve temperature sensing by monitoring the temperature-dependent green UC emission intensity due to the close energy separation between $^2H_{11/2}$ and $^4S_{3/2}$, which allows the $^2H_{11/2}$ level to be thermally populated by the $^4S_{3/2}$ level, which results in variation in the transitions of $^2H_{11/2} \rightarrow {}^4I_{15/2}$ and $^4S_{3/2} \rightarrow {}^4I_{15/2}$ of Er^{3+} in the presence of a temperature change. The FIR of the green UC emissions at 528 nm and 549 nm is described by Eq. (1):

$$\mathrm{FIR} = \frac{I_{528}}{I_{549}} = \frac{N(^2H_{11/2})}{N(^4S_{3/2})} = \frac{g_H \sigma_H \omega_H}{g_S \sigma_S \omega_S} \exp\left[-\frac{\Delta E}{k_B T}\right] = C \exp\left[-\frac{\Delta E}{k_B T}\right], \quad (1)$$

where N, g, σ, and ω, are the number of ions, degeneracy of each level, emission cross section, and angular frequency of the fluorescence transitions from the $^2H_{11/2}$ and $^4S_{3/2}$ levels to the $^4I_{15/2}$ level, respectively. ΔE is the energy gap between the $^2H_{11/2}$ and $^4S_{3/2}$ levels, k_B is the Boltzmann constant, and T is the absolute temperature. The pre-exponential constant is given as $g_H \sigma_H \omega_H / g_S \sigma_S \omega_S$. S, the absolute thermal sensitivity, is used to evaluate the performance of temperature sensing based on the FIR technique and calculated as Eq. (2) [25]:

$$S = \frac{dR}{dT} = \mathrm{FIR}\left(\frac{\Delta E}{k_B T^2}\right). \quad (2)$$

The experimental setup used for temperature-sensing testing is shown in Fig. 5. Pump light was provided from a 980 nm laser diode (MCSPL-980, MC Fiber Optics, China) that was transmitted via the MMF to the three cores suspended on the inner wall of the STCHF to couple into the microsphere and absorbed by the Er^{3+} and Yb^{3+} to emit the strong green light output. An optical probe of the miniature spectrometer (USB4000, Ocean Optics, China) was fixed above the microsphere to detect the UC fluorescence of the microsphere, and the emission spectrum was obtained by processing the collected signals using computer software provided with the instrument (Ocean View). The fiber structure was placed in a grooved temperature-controlled console to uniformly heat the fiber.

The UC luminescence of the microsphere was initially measured at different pump powers at room temperature, and the result is shown in Fig. 6. Unfortunately, there exists a little higher loss of the pump light entering the STHCF via the MMF than in the case of a traditional taper-fiber-coupling microsphere structure, and the sensitivity of the detector is not high, so that little UC luminescence of the microspheres was detected until the input power reached 50 mW. The change of the green light emission intensity of the microspheres as a function of temperature was also measured, and the results

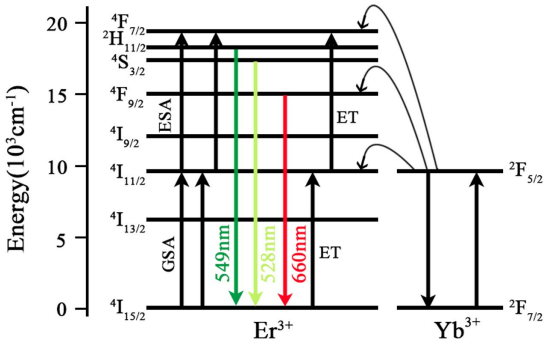

Fig. 4. Energy-level diagram of the UC emissions for the Er^{3+}-Yb^{3+} co-doped tellurite glass under 980 nm laser excitation.

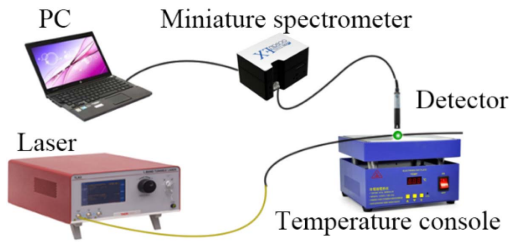

Fig. 5. Experimental setup used for temperature-sensing testing.

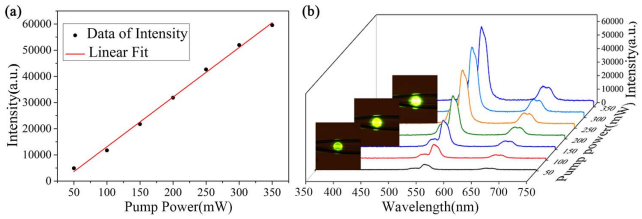

Fig. 6. (a) Linear fit of UC luminescence intensity of the microsphere at different pump powers at room temperature; (b) UC luminescence spectra; insets: micrographs of the microsphere-emitting light at different pumps.

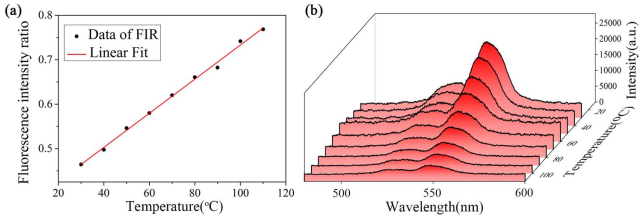

Fig. 7. (a) Linear fit of UC luminescence intensity ratio; (b) UC luminescence spectra of the microsphere at different temperatures.

are shown in Fig. 7. During the measurement process, the laser was not turned on all the time. After each temperature measurement step, the laser was turned off until measuring the next temperature, so as to avoid the destruction of the UC luminescence caused by the thermal effect of laser irradiation. The absolute sensitivity was calculated according to Eq. (1), and the maximum sensitivity value was determined as 5.47×10^{-3} K^{-1} at 383 K. The sensor offers a competitively higher sensitivity compared to other temperature-dependent FIR-based sensors [16–18].

A large volume of high-Q-factor ($\sim 10^4$) Er^{3+}-Yb^{3+} co-doped tellurite glass microspheres have been successfully fabricated using the powder floatation method in a single-batch process. Furthermore, a specially designed STCHF as part of a novel fiber structure based on SMF-MMF-STCHF-MMF-SMF has been successfully implemented to deliver a robust, high-intensity green light source, and a microsphere was successfully placed inside the hollow fiber. The 980 nm pump light was coupled from the suspended cores into the microsphere, and the dopant ions in the microsphere were excited so as to cause the Er^{3+} ions to undergo energy level transitions, and thus a strong UC green light emission was emitted. A maximum temperature sensitivity of 5.47×10^{-3} K^{-1} was measured at 383 K, which compares favorably with similar devices referenced in the literature. It is worth noting that by adjusting the fiber structure to reduce transmission loss and increase the evanescent field, it is also expected that lasing could be achieved, which offers great application potential for integrated laser devices.

Funding. National Natural Science Foundation of China (NSFC) (61575050); National Key R&D Program (2016YFE0126500); Fundamental Research Funds for the Central Universities (HEUCFG201841); Open Fund of the State Key Laboratory on Integrated Optoelectronics (SKLIOE) (IOSKL2016KF03); "111" Project to the Harbin Engineering University (B13015); Key Program for Natural Science Foundation of Heilongjiang Province of China (ZD2026012).

REFERENCES

1. J. Roman, P. Camy, M. Hempstead, W. Brocklesby, S. Nouh, A. Beguin, C. Lerminiaux, and J. Wilkinson, Electron. Lett. **31**, 1345 (1995).
2. L. Aigouy, G. Tessier, M. Mortier, and B. Charlot, Appl. Phys. Lett. **87**, 184105 (2005).
3. R. G. Smart, D. C. Hanna, A. C. Tropper, S. T. Davey, S. F. Carter, and D. Szebesta, Electron. Lett. **27**, 14 (1991).
4. A. Mori, Y. Ohishi, and S. Sudo, Electron. Lett. **33**, 10 (1997).
5. L. Hai, J. Shibin, W. Jianfeng, S. Feng, P. Nasser, and E. Y. B. Pun, J. Phys. D **36**, 7 (2003).
6. A. K. Kewell, G. T. Reed, and F. Namavar, Sens. Actuators A Phys. **65**, 160 (1998).
7. Z. P. Cai and H. Y. Xu, Sens. Actuators A Phys. **108**, 187 (2003).
8. D. Jaque and F. Vetrone, Nanoscale **4**, 4301 (2012).
9. G. Maciel, L. D. S. Menezes, A. Gomes, C. B. D. Araújo, Y. Messaddeq, A. Florez, and M. A. Aegerter, IEEE Phot. Technol. Lett. **7**, 12 (1995).
10. S. F. León-Luis, U. R. Rodríguez-Mendoza, P. Haro-González, I. R. Martín, and V. Lavín, Sens. Actuators B Chem. **174**, 176 (2012).
11. J. Sokolnicki, Mater. Chem. Phys. **131**, 306 (2011).
12. S. A. Wade, S. F. Collins, and G. W. Baxter, J. Appl. Phys. **94**, 4743 (2003).
13. B. Lai, L. Feng, J. Wang, and Q. Su, Opt. Mater. **32**, 1154 (2010).
14. P. V. D. Santos, M. T. D. Araujo, A. S. Gouveia-Neto, J. A. M. Neto, and A. S. B. Sombra, IEEE J. Quantum Electron. **35**, 3 (1999).
15. Y. Tian, Y. Tian, P. Huang, L. Wang, and Q. Shi, Chem. Eng. J. **297**, 26 (2016).
16. N. Vijaya, P. Babu, V. Venkatramu, C. Jayasankar, S. León-Luis, U. Rodríguez-Mendoza, I. Martín, and V. Lavín, Sens. Actuators B Chem. **186**, 156 (2013).
17. A. Pandey, S. Som, V. Kumar, V. Kumar, K. Kumar, V. K. Rai, and H. Swart, Sens. Actuators B Chem. **202**, 1305 (2014).
18. S. F. León-Luis, U. R. Rodríguez-Mendoza, E. Lalla, and V. Lavín, Sens. Actuators B Chem. **158**, 1 (2011).
19. D. Manzani, J. F. da Silveira Petruci, K. Nigoghossian, A. A. Cardoso, and S. J. Ribeiro, Sci. Rep. **7**, 45196 (2017).
20. F. Vanier, F. Côté, M. E. Amraoui, Y. Messaddeq, Y.-A. Peter, and M. Rochette, Opt. Lett. **40**, 5227 (2015).
21. Z. Yang, Y. Wu, X. Zhang, W. Zhang, P. Xu, and S. Dai, IEEE Photon. Technol. Lett. **29**, C1 (2017).
22. L. de Sousa-Vieira, S. Ríos, I. R. Martín, L. García-Rodríguez, V. N. Sigaev, V. I. Savinkov, and G. Yu Shakhgildyan, Opt. Mater. **83**, 207 (2018).
23. M. Zhang, W. Yang, K. Tian, J. Yu, A. Li, S. Wang, E. Lewis, G. Farrell, L. Yuan, and P. Wang, Opt. Lett. **43**, 16 (2018).
24. B. Dong, D. P. Liu, X. J. Wang, T. Yang, S. M. Miao, and C. R. Li, Appl. Phys. Lett. **653**, 18 (2007).
25. S. F. Collins, G. W. Baxter, S. A. Wade, T. Sun, K. T. V. Grattan, Z. Y. Zhang, and A. W. Palmer, J. Appl. Phys. **84**, 4649 (1998).